

Article

Hand Movement Classification using Burg Reflection Coefficients

Daniel Ramírez-Martínez¹, Mariel Alfaro-Ponce² , Oleksiy Pogrebnyak^{1,†} , Mario Aldape-Pérez³  and Amadeo-José Argüelles-Cruz^{1,*} 

¹ Centro de Investigación en Computación, Instituto Politécnico Nacional. Av."Juan de Dios Bátiz" s/n esq. Miguel Othón de Mendizábal, Col. Nueva Industrial Vallejo, Del. Gustavo A. Madero, Ciudad de México; dhanielrhamirez@gmail.com; oleksiy@cic.ipn.mx; jamadeo@cic.ipn.mx

² Departamento de Ciencias e Ingenierías, Universidad Iberoamericana Puebla. Blvrd del Niño Poblano 2901, Reserva Territorial Atlixcáyotl, Centro Comercial Puebla, 72810 San Andrés Cholula, Pue. México; marielalfa@gmail.com

³ Centro de Innovación y Desarrollo Tecnológico en Cómputo, Av."Juan de Dios Bátiz" s/n esq. Miguel Othón de Mendizábal, Col. Nueva Industrial Vallejo, Del. Gustavo A. Madero, Ciudad de México, C.P. 07700.; maldape@ipn.mx

* Correspondence: jamadeo@cic.ipn.mx; Tel.: +52-55-5729-6000 ext.56593

|| † In Memoriam

Version October 29, 2018 submitted to Preprints

Abstract: Classification of electromyographic signals has a wide range of applications, from clinical diagnosis of different muscular diseases to biomedical engineering, where their use as input control of prosthetic devices has become a hot topic of research. Challenge of classifying this signals relies on the accuracy of the proposed algorithm and the possibility of its implementation on hardware. This paper consider the problem of electromyography signal classification, solved with the proposed signal processing and feature extraction stages, with focus lying on the signal model and time domain characteristics for better classification accuracy. The proposal considers a simple preprocessing technique that produces signals suitable for feature extraction, and the Burg reflection coefficients to form learning and classification patterns. These coefficients yield a competitive classification rate compared to used time domain features. Sometimes, the feature extraction from electromyographic signals showed that procedure can omit less useful traits for machine learning models. Using feature selection algorithms provides a higher classification performance with as fewer traits as possible. Algorithms achieved a high classification rate up to 100% with low pattern dimensionality, with other kinds of uncorrelated attributes for hand movement identification.

Keywords: Electromyography, Hand Movement, Health Monitoring, Maximum Entropy Reflection Coefficients, Classification Algorithms, Machine Learning, Feature Selection.

1. Introduction

Electromyography (EMG) is an electrodiagnostic medical procedure to assess the health of muscles and the nerves cells that controls them, with the detection, recording and analysis of electromyography signals (sEMG). The EMG provide physicians and health experts with the information generated by the muscle contractions, that is the ionic flow through the muscle fibre [1]. Research has considered EMGs as an important field of study due to the diversity of its applications in clinical medicine and biomedical engineering [2]. EMG has applications such as the diagnosis of nervous system disorders and muscular diseases like myopathies detection and neuropathies [3–5]. All these applications need preprocessing of signals and its extraction of features [6]. sEMG are useful as input control signals for prosthetic limbs [7,8], in rehabilitation as a measurement parameter of muscular effort [9], and for the development of muscle machine interfaces [10].

Most EMG applications involves real-time systems, that are needed to run with low-cost computational features [11]. As a matter of the fact, in the development of prosthetic, orthotic and

30 rehabilitation devices the EMG can be employed as a part of the control system. In the results reported
31 by [12] EMG pattern recognition and myoelectric control are compared for prosthetic control, the
32 paper remarks that these signals are suitable for the control with highlights in the implementations of
33 algorithms that are capable to distinguish between signals that have similarities. These similarities are
34 presented in users that have lost a body part, as a consequence of the absence of peripheral structures
35 in the musculoskeletal system, where the classification of EMGs features become a challenge. The
36 most used EMGs features are time domain attributes [13] that can be obtain by root-mean-square
37 value (RMS), mean average value (MAV), variance (VAR), Willison amplitude (WAMP), wavelength
38 (WL), and many others [14] [15]. These characteristics have been used in different classification tasks,
39 and the classification rate increases with the use of a proper signal preprocessing stage; for instance,
40 Chowdhury et al. consider the use of wavelet and empirical mode decomposition, first differentiation
41 or independent component analysis in [15]. Despite the performances achieved at the preprocessing
42 stage, computational complexity might increase adding a delayed response. Several authors use
43 autoregressive models and the characteristics of random processes, such as first and second moments
44 and others, in tasks related with classification of myopathy or neuropathy diseases. For example,
45 Bozkurt et al. report 97% in performance using fifteenth order autoregressive models (AR) Yule-Walker,
46 Burg, Covariance, Modified Covariance and subspace base methods to extract features from 1200
47 sEMG, applying high resolution and high sampling rate in invasive electrodes implanted in a Bicep
48 brachii muscle [16].

49 In a different research dedicated to the hand movement, Phinyomark et al. report a high
50 classification rate of 97.76%, achieved by applying a quadratic discriminant analysis and four AR
51 coefficients per channel and including a preprocessing stage whose output is the first differentiation
52 of sEMG [17]. They extracted information from the activity of five forearm muscles: WL, difference
53 absolute mean value (DAMV), difference absolute standard deviation value (DASDV), difference
54 absolute variance (DVARV), difference absolute standard deviation (DASDV), second order moment
55 (M2), WAMP, integrated EMG (IEMG), MAV. They used also these features in their previews works [18].
56 Simple squared integration SSI, VAR, RMS, myopulse percentage rate (MYOP), cepstral coefficients
57 (CC), log detector (LOG), temporal moment (TK) and v order (V) with another point of view in [17]
58 applying the seventh order Daubechies mother wavelet and the four decomposition levels before
59 sEMG characterisation extracts RMS and MAV. They test the behaviour of these traits to estimate
60 whether they are useful for identification of six daily hand movements monitoring flexor and extensor
61 carpi radialis longus muscles.

62 Liu et al. describe the use of an assemble classifier of support vector machines (SVM) [19],
63 classifying eight different hand grasps with a precision rate of 93.54%; extracting sEMG from three
64 different forearm muscles and fourth order AR coefficients and HEMG builds the feature vector per
65 channel. In their work the aim is to get significant features and a classification model that permits
66 increasing the classification rate of sEMG. However, assembling SVM models results computationally
67 expensive. Angari et al. consider fifteen channels to digitalise sEMG and to characterise five hand
68 movements, where they extract twenty-one attributes per channel (MAV, WL, ZC, SSC, AR6, and
69 others) to implement feature selection methods and channel discrimination [20]. In this case, the aim
70 of the research was to train the SVM with low dimensionality patterns and the most representative
71 forearm muscles; this work concludes that MAV and WL are appropriate for classification tasks.

72 The method of Khezri et al. uses an adaptive neuro-fuzzy inference system to test its classification
73 rate in a six hand movement dataset containing four channels [21]. The considered features are MAV,
74 SSC, ZC, and 10 order AR model coefficients. Merging these attributes to create patterns for sEMG
75 representation provokes that classification rates runs from 86% to 100%.

76 Ruangpaisarn et al. present a feature extraction technique for hand movement classification,
77 considering two pairs of EMG electrodes and the merging and transformation of both channels
78 into a squared matrix to perform factorisation via singular value decomposition [22]. They report
79 the use of singular values in the matrix main diagonal and the training of SVM with fifty feature

80 instances, achieving a performance of 98.22%. The issue in this work comprises taking samples where
 81 no muscular activity is looked at, and working with a 2D vector in most cases leads to non-linear
 82 computational complexity. With the same dataset, Sapsanis et al. used a preprocessing stage in which
 83 signals are 3 level decomposed with empirical mode decomposition, so that noise is reduced [23].
 84 For each decomposition level and raw sEMG, they extract the following attributes: IEMG, ZC, VAR,
 85 SSC, WL, WAMP, kurtosis and skewness. With a linear discrimination analysis, a rate of correct
 86 classifications reaches 89.21%.

87 The resumes in [14] and [15] show the variety of features for classifying sEMG and preprocessing
 88 techniques that might lead to a classification model performance increasing. However, none of the
 89 studies use the reflection coefficients as features for pattern recognition.

90 The aim of this work is to develop a classification algorithm for sEMG with low computational
 91 cost and with a competitive classification rate. The remainder of this paper present the following
 92 distribution: Section 2 describe the hand movement database that was employed, also a brief resume
 93 of the signal preprocessing techniques and different features useful for classification are described.
 94 Then, the proposed classification method is presented. Section 3 shows the results obtained by the
 95 classification technique. Section 4 and 5 are the discussion and conclusion of the results achieved by
 96 the proposed methodology for sEMG classification.

97 2. Materials and Methods

98 2.1. Data selection and preprocessing

99 We used an EMG dataset from the University of California in Irving (UCI) machine learning
 100 repository, the same as in [22] and [23]. The data describes six different hand movements taken from
 101 Flexor Capri Ulnaris and Extensor Capri Radialis muscles of five healthy people (three women and
 102 two men) who performed with no restrictions thirty times each hand action during 6 seconds each;
 103 signal sampling frequency is 500Hz. The dataset contains 1800 time series available to classify 6 hand
 104 grasps (Spherical, Tip, Palmar, Lateral, Cylindrical and Hook).

105 Before feature extraction, there is a simple preprocessing treatment applied to each signal. At
 106 the first preprocessing stage, the method eliminate the initial samples, where muscle activation is
 107 absent and only noise is present, to avoid the feature extraction lacking the phenomena information.
 108 The next step comprises the extract of the signal-mean-value at all data points; this operation
 109 is important to comply with the restrictions imposed by the optimal linear filtering theory [24].
 110 Linear prediction model framework requires restrictions such as autoregressive models. Otherwise,
 111 performing classification/prediction models might decrease. Here, we used the simple arithmetic
 112 mean value computed as

$$\mathbf{x} = \frac{1}{N} \sum_{n=0}^N x[n] \quad (1)$$

113 where \mathbf{x} is the mean value; $x[n]$ is EMG signal and N is the total number of samples. The
 114 application of the mean (1) implies a new sample value which is described as $\bar{x}[n] = x[n] - \bar{x}$
 115 $1 \leq n \leq N$. Figure 1 illustrates the proposed preprocessing stages.

116 These two conditioning steps have linear complexity and supply feature extraction stage with an
 117 appropriated sEMG.

118 2.2. Standard time domain features

119 The integrated EMG feature is defined as the cumulative addition of each signal sample absolute
 120 value:

$$IEMG = \sum_{n=0}^N |x_n| \quad (2)$$

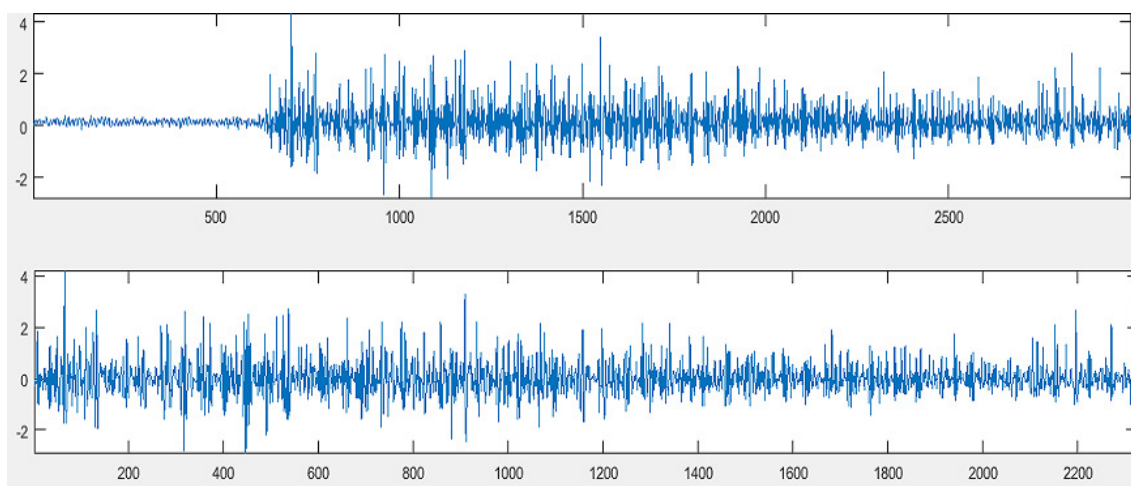


Figure 1. On top original signal, on bottom clipped signal with zero mean value.

where other attribute is mean absolute value; it is one of the most useful attributes in many researches and consists of computing the mean absolute amplitude value of sEMG:

$$MAV = \frac{1}{N} \sum_{n=0}^N |x_n| \quad (3)$$

121 The simple squared integration feature describes the energy of sEMG and is mathematically
122 defined as cumulative addition of absolute squared value of each sample:

$$SSI = \sum_{n=1}^N |x_n|^2 \quad (4)$$

123 A stochastic process as a sEMG can be defined by its first and second order moment, i.e., mean and
124 variance values. Therefore, these features might be part of the pattern. The mathematical definition for
125 the variance takes considers a sEMG is a near to zero mean process, so its definition becomes:

$$VAR = \frac{1}{N-1} \sum_{n=1}^N x_n^2 \quad (5)$$

126 The root mean squared value (RMS) reveals the information of the amount of strength yield by a
127 muscle, and is defined as the square root of the mean squared values. In many research works, this
128 attribute is considered important for different tasks:

$$RMS = \sqrt{\frac{1}{N} \sum_{n=1}^N x_n^2} \quad (6)$$

129 The wave length is a distance between a pair of adjacent samples along all sEMG:

$$WL = \sum_{n=1}^N |x_{n+1} - x_n| \quad (7)$$

130 The zero crossing feature describes the number of times that the sEMG amplitude becomes
131 positive or negative. Its definition considers a threshold whose aim is to count only the events
132 produced by muscular activity:

$$ZC = \sum_{n=1}^{N-1} [sgn(x_n \times x_{n+1}) \cap |x_n - x_{n+1}| \geq 0], sgn(x) = \begin{cases} 1, & x \geq threshold \\ 0, & otherwise \end{cases} \quad (8)$$

133 The slope sign attribute considers three adjacent samples to determine the number of times that a
134 slope sign between these sEMG values changes:

$$SSC = \sum_{n=2}^N f((x_n - x_{n-1}) \times (x_n - x_{n+1})), f(x) = \begin{cases} 1, & f = th \\ 0, & otherwise \end{cases} \quad (9)$$

135 where th is a threshold.

136 The quantity of motor unit action potential is estimated through the Willison amplitude counting
137 the number of times that two adjacent samples overcome a threshold reducing artifacts produced by
138 noise:

$$WAMP = \frac{1}{N} \sum_{n=1}^N f(|x_n|), f(x) = \begin{cases} 1, & x \geq th \\ 0, & otherwise \end{cases} \quad (10)$$

139 The amount of muscular pulses is described by the log detector which uses a threshold to avoid
140 noisy samples.

$$MYOP = \frac{1}{N} \sum_{n=1}^N f(|x_n|), f(x) = \begin{cases} 1, & x \geq th \\ 0, & otherwise \end{cases} \quad (11)$$

141 2.3. Autoregressive model features

142 A linear autoregressive model describes a random process using p coefficients [24]. The goal
143 consists in extracting p coefficients to construct a representation of each sEMG sample $x[n]$ with the
144 preceding signal values ($x[n-1], x[n-2], \dots, x[n-p]$) making a linear combination, which carries an
145 error or white noise term:

$$x[n] = \sum_{k=1}^p a_k x[n-k] + e[n] \quad (12)$$

146 where $x[n]$ is the generated sEMG value through k earlier samples $x[n-k]$, p is the order of the
147 model, $e[n]$ expresses an added error or white noise term and a_k is the autoregressive coefficients. The
148 mathematical approach used to derive the autoregressive coefficients defines the regressive model
149 type. The most popular autoregressive model is the Yule-Walker model that uses the estimated values
150 of the correlation function calculated as:

$$\hat{r}_{xx}(n, n-k) = Ex(n)x(n-k)k = 0, \pm 1, \pm 2, \dots \quad (13)$$

151 Having \hat{r}_{xx} estimated with (13), a $N \times N$ squared Yule-Walker matrix equation is built as follows:

$$\begin{bmatrix} \hat{r}_{xx}(0) & \hat{r}_{xx}(-1) & \dots & \hat{r}_{xx}(-p) \\ \hat{r}_{xx}(1) & \hat{r}_{xx}(0) & \dots & \hat{r}_{xx}(-p+1) \\ \vdots & \vdots & \dots & \vdots \\ \hat{r}_{xx}(p) & \hat{r}_{xx}(p-1) & \vdots & \hat{r}_{xx}(0) \end{bmatrix} \begin{bmatrix} 1 \\ a_1 \\ \vdots \\ a_p \end{bmatrix} = \begin{bmatrix} \sigma_w^2 \\ \hat{r}_{xx}(1) \\ \vdots \\ \hat{r}_{xx}(p) \end{bmatrix} \quad (14)$$

152 where σ_w^2 is the variance of the modelled stochastic process. As the correlation matrix describes
153 an equation system and fulfils Toeplitz definition, the method use the recursive Levinson-Durbin
154 algorithm to get the autoregressive coefficients a_p .

155 Following a different approach, the Burg maximal entropy method, in [24] and [25] proposes the
156 expansion of \hat{r}_{xx} , adding $\hat{r}_{xx}(p+1), \hat{r}_{xx}(p+2), \hat{r}_{xx}(p+3), \dots$. With this consideration in mind, the method
157 extrapolate the new correlation values, maximising the entropy between them, so their randomness
158 is high. The extrapolation of autoregressive series changes the predictions of backward and forward
159 signal values $\hat{x}(n)$ and $\hat{x}(n-m)$:

$$\hat{x}(n) = \sum_{k=1}^m a_m(k)x[n-k], 0 \leq k \leq m-1, m = 1, 2, \dots, p \quad (15)$$

$$\hat{x}(n-m) = - \sum_{k=1}^m (a_m)^*(k)x[n+k-m], 0 \leq k \leq m-1, m = 1, 2, \dots, p \quad (16)$$

160 where $a_m(k)$ is k -th autocorrelation coefficient of the model of order m , which implies a
161 combination of previous values and the reflection coefficients K_m [24]:

$$a_m(k) = a_{m-1}(k) + k_m(a_{m-1})^*(m-k), 1 \leq k \leq m-1, 1 \leq m \leq p \quad (17)$$

162 The Burg proposal produces good results for different distributions; when the stochastic process
163 has a Gaussian distribution, both autoregressive methods yield the same coefficient values [24].

164 2.4. Dataset construction

165 To develop and test the proposed approach for hand movement classification, the features
166 described above are first extracted from different channels $S_{Ch1}[n], \dots, S_{Chk}[n]$ and placed in a dataset.
167 Each feature extractor (see Figure 2) forms single or multiple features and its output is a vector
168 that represents a pattern of the form $P_{Chk}[n] = [feature_{1chk}, feature_{2chk}, \dots, feature_{Nchk}]$. Next, the
169 derived features from the channels are transferred to the pattern builder that concatenates the instances
170 to generate an object containing the extracted features, and a label assigned for the class instances
171 $P_i[n] = [P_{Ch1}[n], P_{Ch2}[n], \dots, P_{Chk}[n], classlabel]$. Figure 2 shows the dataset building block diagram.

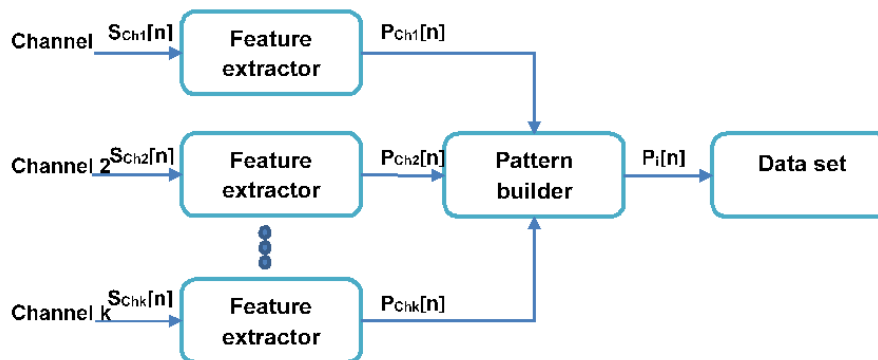


Figure 2. Data set building block diagram.

172 2.5. Proposed classification methodology

173 2.5.1. Burg reflection coefficients

174 As mentioned in Section 2.3, Burg autoregressive model introduces the forward and backward
175 prediction errors

$$f_m(n) = x(n) - \hat{x}(n), b_m(n) = x(n-m) - \hat{x}(n-m) \quad (18)$$

176 These errors are defined by the following recursive renovation equations of lattice linear prediction
177 filter

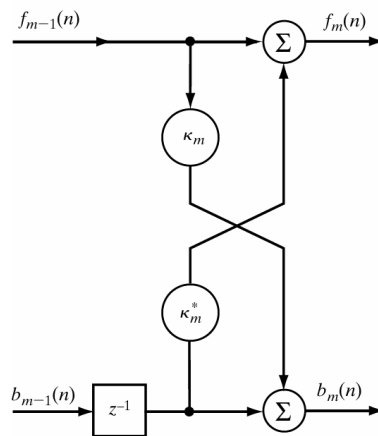


Figure 3. Lattice filter prediction cascade diagram.

$$\begin{aligned}
 f_0(n) &= b_0(n) = x(n), \\
 f_m(n) &= f_{m-1}(n) + K_m b_{m-1}(n-1) \quad m = 1, 2, \dots, p, \\
 b_m(n) &= K_m^* f_{m-1}(n) + b_{m-1}(n-1) \quad m = 1, 2, \dots, p
 \end{aligned}
 \tag{19}$$

178 The least squared error is

$$\varepsilon_m = \sum_{n=m}^{N-1} [|f_m(n)|^2 + |b_m(n)|^2]
 \tag{20}$$

179 Minimizing expression 20, the reflection coefficients are obtained [24]:

$$K_m^* = \frac{-\sum_{n=m+1}^{N-1} f_{m-1}(n) b_{m-1}^*(n-1)}{\frac{1}{2} \sum_{n=m+1}^{N-1} [|f_m(n)|^2 + |b_m(n)|^2]}, \quad m = 1, 2, \dots, p
 \tag{21}$$

180 Reflection coefficients are the harmonic mean value of backward and forward error coefficient
 181 cross correlation. The numerator is the cross correlation of the prediction errors and the denominator is
 182 the smallest square estimation of these errors, so, $|K_m| \leq 1$. The reflection coefficients (21) are computed
 183 iteratively through the signal values; this is the reason they are proposed as features for classification
 184 tasks as their complexity is linear, and there is no evidence of their usage in such tasks.

185 2.5.2. Classification model training

186 Classification models involved in this research work are Bayesian, K nearest neighbor, multilayer
 187 perceptron, decision trees and support vector machines with different kernels. These classifiers are
 188 available in machine learning tool WEKA [26] and were taken with the purpose of evaluating their
 189 performance using different sEMG features. For the training phase, the following three datasets were
 190 generated comprising 900 instances and 10 traits per channel:

- 191 • Time domain Data set (1)-(11): TD=[IEMG MAV SSI VAR RMS WL WAMP SSC ZC MYOP]
- 192 • Burg autoregressive coefficients (17): Arb=[Arb₁ Arb₂ ... Arb_n]
- 193 • Reflection coefficients: K=[K₁ K₂ ... K_n]

194 The classification algorithms were trained once, and the performance was obtained by K -fold
 195 cross validation with K value of 10 because they widely use it in state-of-the-art related works, and the
 196 datasets lack of class unbalance. Moreover, each instance takes part in the training and testing set for
 197 a single run of the learning algorithm. Burg autoregressive coefficients (17) were chosen instead of
 198 Yule-Walker autoregressive coefficients (14) because different distributions of the Burg model produces

199 a more accurate approximation [24]. After classifying three main datasets, K, Arb and TD features were
 200 joined into a new dataset with patterns of the form of $X = [IEMG\ MAV\ SSI\ VAR\ RMS\ WL\ WAMP$
 201 $SSC\ ZC\ MYOP\ Arb_1\ Arb_2 \dots Arb_n\ K_1\ K_2 \dots K_n]$; in order to evaluate how the interaction between
 202 these different features is reflected in classification model performance.

203 2.5.3. Feature selection

204 Under the same validation method (k-fold cross validation), taking the dataset with instances in
 205 the form of X, WEKA principal components (PC) and subset evaluation (SE) feature selection models
 206 [26] applied to reduce the pattern dimensionality and select the less redundant and correlated attributes
 207 for the classification task. Feature selection guarantees a reduction in dimensionality with or without a
 208 degradation of the classifier model performance. As observed in Section 2, some time domain features
 209 rely on sEMG amplitude such as RMS and MAV, and others depend on counting a certain event
 210 according to a threshold value. As a result, these attributes might contain a redundancy; also, the Burg
 211 autoregressive coefficients and reflection coefficients are tied according to (17). Sequential forward
 212 selection [27] strategy comprising taking just one of the different features used for dataset construction.
 213 Another feature selection criterion is plus l – take away r algorithm - [27], based on taking l traits
 214 from TD, K and Arb from X and remove the remaining r features, in such a way that the classification
 215 performance remains high. If the exclusion of an attribute causes a lower than previous performance,
 216 the removed sEMG characteristic is returned to the dataset because it is helpful for the class instance
 217 assignment. This process is repeated until the dimensionality cannot be reduced without affecting the
 218 classification rate.

219 3. Results

220 3.1. Datasets classification

221 Here, the results of the hand movement classification with separated datasets are presented. The
 222 parameter changed in SVM model was kernel function. For the rest of models, the default Weka
 223 parameters were not modified. Two values chosen for k in IBk are $k = 1$ and $k = \text{number of classes} + 1$;
 224 assigning $k = 6$ would cause a tie between six classes; the extra value will establish the majority class.
 225 Table 1 describes the results obtained by classifying the hand movements with separated datasets.

Table 1. Classification results of TD, Arb and K datasets separately.

N	features	Bayes		Ik-P 2.0		MLP		Tree		SVM	
		<i>Naive</i>	<i>net</i>	k_1	k_7	–	J48	<i>Random</i>	<i>radial</i>	<i>linear</i>	P3
20	TD	46.55	68.33	93.22	91.22	86.55	83.33	92.88	27.33	76.33	93.11
20	Arb	59.11	63.33	90.77	91.66	86.33	78.00	90.55	47.00	61.11	37.77
20	k	57.44	71.11	93.55	93.33	86.44	74.77	92.00	45.55	65.44	29.77

226 One can observe from Table 1 that TD dataset and the SVM with third order polynomial kernel
 227 (P3 column) gives better decision borders than other kernels. The radial kernel yields the lowest
 228 performance with Bayesian models; whereas the remaining models (trees and MLP) reached high
 229 classification rates, IBk with $k = 1$ obtained the highest. The dataset built only with maximal entropy
 230 autoregressive coefficients (Arb column) is more appropriate to classify with the IBk considering
 231 seven neighbours more than just one. Other learning algorithms such as MLP and decision trees
 232 offer competitive classification rates (78% - 90.77%); Bayesian models overcome linear kernel support
 233 vector machines with a performance of 63.33%. The best performance among the different datasets
 234 is obtained using the reflection coefficient dataset K of the reflection coefficients, classifying 93.55%
 235 of instances using IBk $k = 1$. Despite Bayesian models and SVM still having a low performance, an
 236 improvement in Bayesian net is achieved using the reflection coefficients.

Table 2. Classification performance of combined datasets.

N	features	Bayes		Ik-P 2.0		MLP		Tree		SVM	
		<i>Naive</i>	<i>net</i>	k_1	k_7	–	J48	<i>Random</i>	<i>radial</i>	<i>linear</i>	P3
–	–										
40	$k + TD$	61.44	83.22	99.88	99.55	98.44	87.11	98.33	18.33	83.11	93.22
40	$k + Arb$	78.22	82.33	99.66	99.33	98.44	84.77	98.66	64.00	90.00	54.66
60	X	76.00	83.33	100.0	99.77	99.11	85.55	95.55	17.77	83.00	93.22

237 In Table 2, by merging reflection coefficients and TD features for the training phase (K+TD), most
 238 of the classifiers reach high performance, excluding naïve Bayes and radial kernel SVM. With a 0.22%
 239 classification error, IBk $k = 1$ got the best classification rate above the following models: IBk $k = 7$,
 240 MLP, decision trees and 3th grade polynomial kernel SVM. The resulting dataset of joining the Burg
 241 maximal entropy reflection coefficients, K, and the Burg autoregressive coefficients, Arb, yield patterns
 242 that are best classified by the IBk model with k value of one, slightly above the IBk using $k = 7$, MLP
 243 and random forest. The J48 decision tree and Bayesian models offer high performances and are below
 244 90% accuracy reached by linear kernel SVM; the other kernels have the lowest classification rates.
 245 The combination of all features (TD, Arb, and K) results in a sixty-dimension feature vector, useful to
 246 classify correctly all 900 dataset instances using the IBk with $k = 1$; increasing the number of neighbors
 247 to $k = 7$ decreases the classification rate, but keeps on above the following competitive models, MLP
 248 and random forest. Data distribution does not fit to a radial kernel, therefore, the SVM outputs the
 249 lowest accuracy.

250 3.2. Feature selection classification performance

251 This subsection describes the results of dimensionality reduction trying to reach a higher
 252 classification performance with as fewer traits as possible. After running the feature selection
 253 algorithms, all instances kept on being classified correctly with 20 and 26 features with the nearest
 neighbours and support vector machine models, respectively (see Table 3). SE traits exclude amplitude

Table 3. Classification performances using different feature vectors after feature selection:
 SE=[$Ch_1Arb(1,2,5,9,10)$, $ch_1k(1,2,3,4,9)$, Ch_1WL , Ch_1SSC , Ch_1ZC , Ch_1MYOP , $Ch_2Arb(1,2,4,5,10)$,
 $Ch_2k(1,5,7)$, Ch_2WL , Ch_2MYOP], $FS_1=[ARB(1,2,7,8,10)$, $K(1,2,10)$, ZCC , $MYOP$], $FS_2=[Arb1$, $K1$, ZCC ,
 $RMS]$, $FS_3=[Arb_1$, K_1 , ZCC , $MAV]$, $FS_4=[Arb_1$, K_1 , $MYOP$, $RMS]$ $FS_5=[Arb_1$, K_1 , $MYOP$, $MAV]$.

N	features	Bayes		I-P 2.0		MLP		Tree		SVM	
		<i>Naive</i>	<i>net</i>	k_1	k_7	–	J48	<i>Random</i>	<i>radial</i>	<i>linear</i>	P3
–	–										
26	SE	82.55	91.55	99.88	99.88	99.11	87.77	99.55	18.00	74.33	82.00
26	PC	88.11	88.66	99.66	98.88	97.55	84.11	98.44	100.0	96.11	99.55
20	FS_1	79.88	86.88	100.0	99.66	97.66	86.33	98.77	24.88	68.88	57.77
8	FS_2	64.88	84.22	99.22	99.22	88.55	88.66	97.88	22.33	55.11	49.88
8	FS_3	65.00	83.22	99.22	98.77	89.22	89.55	97.88	22.33	54.33	45.88
8	FS_4	66.77	84.66	98.22	97.77	87.55	88.77	89.88	66.11	70.77	28.66
8	FS_5	67.33	83.00	98.22	97.77	88.55	88.55	98.33	61.44	68.66	32.55

254 related values such as RMS, MAV and so on. They provide high classification rates with the exception
 255 of the linear kernel SVM. The PC dataset was built with the combination of the less correlated features
 256 resulting in a more uniform performance through all tested classifiers, reaching 100% performance
 257 using the SVM with a radial kernel. The FS_1 represents the result of the feature selection process; the
 258 IBk with $k=1$ is still the highest and SVM with any kernel, the lowest. Datasets FS_2 , FS_3 , FS_4 , FS_5 were
 259 obtained taking the first reflection and autoregressive coefficients in combination with MYOP, ZCC,
 260 RMS, MAV. These sets are of low pattern dimensionality and have high performance from 83% up
 261 to 99.22% using the IBk with $k = 1$ (the highest), MLP, decision trees and Bayes net (the lowest); the
 262 remaining models yield a low performance with just 8 attributes.
 263

264 4. Discussion

265 The classification accuracy rate of different learning algorithms depends on the data distribution.
266 This behaviour is expected according to the “no-free-lunch theorems” [28], which state that the best
267 classification model for all datasets does not exist. The justification of why several models have to be
268 compared using the same dataset concurs with that statement.

269 While testing classifiers with separated datasets, Burg reflection coefficients K (21) are more
270 appropriate to be used in conjunction with the Bayes net and IBk models. Since K traits are needed to
271 compute the Burg autoregressive traits, Arb (17), their classification performances are similar. Besides,
272 TD features have different values which rely on amplitude or counting events. Therefore, the MLP,
273 decision trees, and linear and polynomial kernel SVM outputs have high accuracy.

274 Despite the Burg maximal entropy autoregressive and reflection coefficients being closely related,
275 the classification rate increases when these two traits take a part of the dataset. This means that they
276 are not redundant or irrelevant in feature construction tasks; however, as mentioned before, Arb
277 characteristics take more time to be computed because they rely on first computing the reflection
278 coefficients. In addition, as a result of combining three different theoretical frameworks attributes, the
279 highest classification rate is obtained. Hence, a synergy of different attributes is needed for a higher
280 accuracy in the sEMG classification tasks.

281 In Section 3.2, opposite to the results in Table 2, a high classification performance is reached
282 with 26 or fewer features. The fact that the feature vector X has at least 34 redundant or irrelevant
283 traits, which are necessary to be removed using feature selection tools can explain it. As a result,
284 different data distributions are obtained; for instance, principal component analysis performed by
285 WEKA produces a data distribution suitable for the support vector machine with a radial kernel since
286 all patterns are correctly classified.

287 Excluding the PC dataset, the best classifier for the remaining datasets is the IBk model with a
288 different number of neighbours used for class assignment, because the performance of the nearest
289 neighbors-based model depends on k value. For instance, TD and K dataset classification rate decreases
290 as a result of increasing k value, contrasting to what happens with Arb patterns (see Table 1). This
291 behaviour is expected due to the classification phase applying the nearest neighbour to different classes
292 causing in the worst case a tie and a misclassified pattern.

293 The IBk advantage is its simple training phase that bases directly on the dataset compared to
294 Bayesian models that require the computation of probability distributions and cost function. The
295 design of the hidden layer of MLP can be complex and the time of back propagation error reducing
296 might be long. The decision trees as well as multilayer perceptron are hard to design, and they require
297 a pruning process to reduce irrelevant leaves and branches and the SVM has $O(n_3)$ complexity to
298 establish support vectors. The kernel selection and design of the support vectors that best fits the data
299 distribution are needed.

300 An example of kernel selection can be seen from Table 1 with the TD dataset: using the polynomial
301 kernel, a high performance of 93.11% is reached, and merging the TD with K features an improvement
302 of 0.11% is achieved. This is a sign that most of the support vectors are found in the TD traits using
303 such a kernel. Another example is Arb and K traits: they are better classified with a linear kernel, and
304 by joining these two datasets, a considerable increase in the classification rate is obtained (see Table 2)
305 as a consequence of more appropriate data for the support vector estimation.

306 The results that are considered for the discussion are those that was obtained using the same
307 signal dataset; otherwise, any comparison concerning the feature extraction and preprocessing stage
308 based on the classification performance would be unfair.

309 The feature extraction method presented in [22] yields fifty traits and reaches a high performance
310 (98.22%) with no previous signal treatment while the classification rates of 89.21% are obtained with the
311 empirical mode decomposition technique, which denoises the original signal in conjunction with sixty
312 four features proposed in [23]. Our methodology succeeded in classifying all 900 sEMG instances with
313 less than half the features (20 characteristics) than [22] and [23] methods. Their results are exceeded

314 with just 8 traits producing the 99.22% correctly classified signals. Our preprocessing stage consists
315 only in the reduction of noisy samples and the subtraction of the myoelectric signal mean value, which
316 turns out to be effective due to it giving signals suitable to the framework of the developed feature
317 extraction tools, such as Burg reflection coefficients (21).

318 As shown in [23], decomposing sEMG causes an information loss that is reflected in the
319 classification rate; for this reason, all available signal information for the feature extraction task
320 were taken.

321 5. Conclusions

322 The results of hand movement classification of myoelectric signals using different traits have
323 been presented. The Burg linear autoregressive model yields to the reflection coefficients that have
324 been shown to be useful for the sEMG classification; these traits have shown a higher performance
325 that is increased with the standard time domain features and are less complex to compute than the
326 autoregressive coefficients.

327 A high classification rate has been reached using a simple preprocessing stage, which fits the
328 signals to the theory framework in the feature extraction tools. Low pattern dimensionality results from
329 removing redundant traits and building patterns with uncorrelated features such as Burg maximal
330 entropy reflection and autoregressive coefficients and considering different time domain features
331 related to the signal energy and to event counting. Despite a lower feature dimensionality, the
332 classification rate up to 100% has been achieved separately and with other kinds of uncorrelated
333 attributes for the hand movement identification.

334 The applications of the classification technique of signals presented in this work can lead to the
335 possible development of state-of-the-art active prosthetic devices, where the myoelectric classification
336 does not represent a challenge and the implementation of the classification algorithm can be performed
337 in an integrated low cost device.

339 Acknowledgments:

341 This work was partially supported by the Instituto Politécnico Nacional and CONACyT.

343 Conflicts of Interest:

345 The authors declare no conflict of interest.

346 References

- 347 1. De Luca, C.J. Electromyography. In *Encyclopedia of Medical Devices and Instrumentation, Vols 1-4*; John Wiley
348 & Sons, Inc., 2006. doi:10.1002/0471732877.
- 349 2. Raez, M.B.I.; Hussain, M.S.; Mohd-Yasin, F.; Reaz, M.; Hussain, M.S.; Mohd-Yasin, F. Techniques of EMG
350 signal analysis: detection, processing, classification and applications. *Biological procedures online* **2006**.
351 doi:10.1251/bpo115.
- 352 3. Lahmiri, S.; Boukadoum, M. Improved Electromyography Signal Modeling for Myopathy Detection.
353 2018 IEEE International Symposium on Circuits and Systems (ISCAS). IEEE, 2018, pp. 1–4.
354 doi:10.1109/ISCAS.2018.8350893.
- 355 4. Fuglsang-Frederiksen, A. The role of different EMG methods in evaluating myopathy, 2006.
356 doi:10.1016/j.clinph.2005.12.018.
- 357 5. Dostál, O.; Vysata, O.; Pazdera, L.; Procházka, A.; Kopal, J.; Kuchyňka, J.; Vališ, M. Permutation entropy
358 and signal energy increase the accuracy of neuropathic change detection in needle EMG. *Computational*
359 *Intelligence and Neuroscience* **2018**. doi:10.1155/2018/5276161.

- 360 6. Cler, M.J.; Stepp, C.E. Discrete Versus Continuous Mapping of Facial Electromyography for
361 Human-Machine Interface Control: Performance and Training Effects. *IEEE Transactions on Neural Systems
362 and Rehabilitation Engineering* **2015**. doi:10.1109/TNSRE.2015.2391054.
- 363 7. Brunelli, D.; Tadesse, A.M.; Vodermayr, B.; Nowak, M.; Castellini, C. Low-cost wearable multichannel
364 surface EMG acquisition for prosthetic hand control. 2015 6th International Workshop on Advances in
365 Sensors and Interfaces (IWASI). IEEE, 2015, pp. 94–99. doi:10.1109/IWASI.2015.7184964.
- 366 8. Copaci, D.; Serrano, D.; Moreno, L.; Blanco, D.; Copaci, D.; Serrano, D.; Moreno, L.; Blanco, D. A High-Level
367 Control Algorithm Based on sEMG Signalling for an Elbow Joint SMA Exoskeleton. *Sensors* **2018**, *18*, 2522.
368 doi:10.3390/s18082522.
- 369 9. Repnik, E.; Puh, U.; Goljar, N.; Munih, M.; Mihelj, M.; Repnik, E.; Puh, U.; Goljar, N.; Munih, M.; Mihelj, M.
370 Using Inertial Measurement Units and Electromyography to Quantify Movement during Action Research
371 Arm Test Execution. *Sensors* **2018**, *18*, 2767. doi:10.3390/s18092767.
- 372 10. Merletti, R.; Farina, D. *Surface Electromyography: Physiology, Engineering and Applications*; John Wiley &
373 Sons, 2016. doi:10.1002/9781119082934.
- 374 11. Hsueh, Y.H.; Yin, C.; Chen, Y.H. Hardware System for Real-Time EMG Signal Acquisition and
375 Separation Processing during Electrical Stimulation. *Journal of Medical Systems* **2015**, *39*, 88.
376 doi:10.1007/s10916-015-0267-6.
- 377 12. Resnik, L.; Huang, H.; Winslow, A.; Crouch, D.L.; Zhang, F.; Wolk, N. Evaluation of EMG pattern
378 recognition for upper limb prosthesis control: a case study in comparison with direct myoelectric control.
379 *Journal of NeuroEngineering and Rehabilitation* **2018**, *15*, 23. doi:10.1186/s12984-018-0361-3.
- 380 13. Venugopal, G.; Navaneethakrishna, M.; Ramakrishnan, S. Extraction and analysis of multiple time window
381 features associated with muscle fatigue conditions using sEMG signals. *Expert Systems with Applications*
382 **2014**. doi:10.1016/j.eswa.2013.11.009.
- 383 14. Nazmi, N.; Abdul Rahman, M.; Yamamoto, S.I.; Ahmad, S.; Zamzuri, H.; Mazlan, S. A Review of
384 Classification Techniques of EMG Signals during Isotonic and Isometric Contractions. *Sensors* **2016**,
385 *16*, 1304. doi:10.3390/s16081304.
- 386 15. Chowdhury, R.H.; Reaz, M.B.I.; Ali, M.A.B.M.; Bakar, A.A.A.; Chellappan, K.; Chang, T.G. Surface
387 electromyography signal processing and classification techniques. *Sensors (Basel, Switzerland)* **2013**.
388 doi:10.3390/s130912431.
- 389 16. Bozkurt, M.R.; Subaşı, A.; Köklükaya, E.; Yilmaz, M. Comparison of AR parametric methods with
390 subspace-based methods for EMG signal classification using stand-alone and merged neural network
391 models. *Turkish Journal of Electrical Engineering and Computer Sciences* **2016**. doi:10.3906/elk-1309-1.
- 392 17. Phinyomark, A.; Limsakul, C.; Phukpattaranont, P. Application of wavelet analysis in EMG feature
393 extraction for pattern classification. *Measurement Science Review* **2011**. doi:10.2478/v10048-011-0009-y.
- 394 18. Veer, K.; Sharma, T. A novel feature extraction for robust EMG pattern recognition. *Journal of Medical
395 Engineering & Technology* **2016**, *40*, 149–154. doi:10.3109/03091902.2016.1153739.
- 396 19. Liu, Y.H.; Huang, H.P.; Weng, C.H. Recognition of Electromyographic Signals Using Cascaded Kernel
397 Learning Machine. *IEEE/ASME Transactions on Mechatronics* **2007**. doi:10.1109/TMECH.2007.897253.
- 398 20. Al-Angari, H.M.; Kanitz, G.; Tarantino, S.; Cipriani, C. Distance and mutual information methods for EMG
399 feature and channel subset selection for classification of hand movements. *Biomedical Signal Processing and
400 Control* **2016**. doi:10.1016/j.bspc.2016.01.011.
- 401 21. Khezri, M.; Jahed, M. A Neuro-Fuzzy Inference System for sEMG-Based Identification of Hand Motion
402 Commands. *IEEE Transactions on Industrial Electronics* **2011**, *58*, 1952–1960. doi:10.1109/TIE.2010.2053334.
- 403 22. Ruangpaisarn, Y.; Jaiyen, S. SEMG signal classification using SMO algorithm and singular value
404 decomposition. Proceedings - 2015 7th International Conference on Information Technology and Electrical
405 Engineering: Envisioning the Trend of Computer, Information and Engineering, ICITEE 2015, 2015.
406 doi:10.1109/ICITEED.2015.7408910.
- 407 23. Sapsanis, C.; Georgoulas, G.; Tzes, A.; Lymberopoulos, D. Improving EMG based classification of basic
408 hand movements using EMD. Proceedings of the Annual International Conference of the IEEE Engineering
409 in Medicine and Biology Society, EMBS, 2013. doi:10.1109/EMBC.2013.6610858.
- 410 24. Haykin, S.S. *Adaptive filter theory*; Pearson, 2014. doi:10.130901261.
- 411 25. Burg, J.P. Maximum entropy spectral analysis. PhD thesis, Stanford, 1975. doi:doi.wiley.com/ 10.1002/
412 0471667196.ess1570.

- 413 26. Witten, I.H.; Frank, E.; Trigg, L.; Hall, M.; Holmes, G.; Cunningham, S.J. Weka : Practical Machine Learning
414 Tools and Techniques with Java Implementations. Proceedings of the ICONIP/ANZIIS/ANNES'99
415 Workshop on Emerging Knowledge Engineering and Connectionist-Based Information Systems, 1999, pp.
416 192–196. doi:10.1.1.16.949.
- 417 27. Ciaccio, E.J.; Dunn, S.M.; Akay, M. Biosignal Pattern Recognition and Interpretation Systems. *IEEE*
418 *Engineering in Medicine and Biology Magazine* **1994**. doi:10.1109/51.265792.
- 419 28. Wolpert, D.H.; Macready, W.G. No free lunch theorems for optimization. *IEEE Transactions on Evolutionary*
420 *Computation* **1997**. doi:10.1109/4235.585893.

421 **Sample Availability:** Samples of the compounds are available from the authors.